

FINDING THE COEFFICIENTS FOR AN ALGEBRAIC EXPLICIT STRESS MODEL FOR THE CLOSURE PROBLEM IN TURBULENCE FROM DNS RESULTS OF THE SQUARE DUCT

Roney L. Thompson, rthompson@mec.uff.br

Grupo de Escoamento de Fluidos Complexos - LMTA - PGMEC - Department of Mechanical Engineering, Universidade Federal Fluminense, Rua Passo da Pátria 156, Niteroi, RJ 24210-240, Brazil

Gilmar Mompean, Gilmar.Mompean@polytech-lille.fr

Laurent Thais, Laurent.Thais@polytech-lille.fr

Université des Science et Technologies de Lille, Polytech'Lille, Laboratoire de Mécanique de Lille, UMR-CNRS 8107, Cité Scientifique, 59655 Villeneuve d'Ascq Cedex, France

Abstract. *Turbulent models provide closure equations that relate the Reynolds stress with kinematic tensors. In this study, we have developed a methodology to quantify the dependence of the Reynolds stress tensor on mean kinematic tensor basis. The analysis is conducted in three steps. In the first approach, one extracts from the anisotropic Reynolds stress tensor, the part that is proportional to the strain rate tensor. The second approach extracts from the anisotropic Reynolds stress tensor the part that is in-phase (coaxial) with the strain rate. The third one, expresses the out-of-phase part as a function of a persistence-of-straining tensor (Thompson and de Souza Mendes, 2005). The study is conducted for the turbulent flow through a square duct using DNS (direct numerical simulation) data. As expected for this anisotropic complex flow, the results have shown that the tensorial form of the Boussinesq hypothesis is not a good assumption even for the region far from the wall. We then show that the set of tensor basis composed by the rate-of-strain tensor, its square, and the persistence-of-straining tensor is able to describe well the anisotropic Reynolds stress (up to 90% of it). With the proposed methodology, the scalar coefficients of nonlinear algebraic turbulent models can be determined.*

Keywords: *AESM models, Tensor decomposition, DNS square duct*

1. INTRODUCTION

In order to predict a turbulent flow in the framework of a Reynolds Averaged Navier-Stokes (RANS) approach, the development of a turbulent constitutive equation has been a subject of intense research over the last three past decades. This constitutive equation is necessary as a single-point turbulent closure model to obtain the Reynolds stress tensor. Over this period, a significant number of closures schemes have been proposed ranging from the full differential transport equations to the simple algebraic specification using the turbulent velocity and length scales. The simplest one, the model using a linear relationship between the Reynolds stress and the mean strain rate through an eddy viscosity proposed by Boussinesq (1877), has been employed in several computations fluid dynamics (CFD) simulations with some success for wall boundary layers. Even though, wall functions have been developed to correct this model in the near wall region (viscous sub-layer and buffer layer). Since the pioneer works of Lumley (1970) and Pope (1975) proposing non-linear eddy viscosities, the limitation of the linear model is known for modeling more complex turbulent flows as jets, flow over curved surfaces, secondary flows, etc.

On the other hand, high-order models, where closures are needed for the pressure-strain rate correlations and for the triple-fluctuation-velocity correlation to solve the partial differential equations for each component of the Reynolds stress tensor can better represent the physics of the turbulence. However, the development of such models requires more detailed knowledge of turbulence in order to develop closures for several unknown terms present in the differential equation for the Reynolds stress.

Concerning the single-point turbulent closure model to obtain the Reynolds stress tensor, an intermediate level of closure complexity that retain a good level of the predictability capacity of the full differential equations for the Reynolds stress requires additional assumptions on the nature of the turbulent flow being considered. A hypothesis widely used on constructing these *nonlinear eddy viscosity models* (NLEVMs) is the weak equilibrium condition on the turbulent Reynolds stress which was formulated by Rodi (1972,1976) as

$$\frac{Db}{Dt} = 0 \quad (1)$$

In this level, the Boussinesq-type eddy viscosity is replaced by higher-order expansion terms of powers of the mean strain rate and rotation rate tensors. In this kind of approach the model is also coupled through the production term of turbulent energy, using the two-equation formulation for two turbulent scales, the kinetic energy (k) and its rate of dissipation ϵ . These models retains the differential features of the two-equation formulation and some degree of Reynolds stress anisotropy due to the higher-order terms. This level of closure is known as *nonlinear eddy viscosity models*

(NLEVMs). As shown by Gatski and Jongen (2000), this class of models can be seen as a “most” general expression form of the eddy viscosity (for example the model of Speziale (1987)). Within this class of models lies the the group of algebraic stress models (ASM), which are more closely related to the full differential Reynolds stress closure. The solution of tensorial equation, using a set of basis tensors, allows to represent the Reynolds stress as a function of the kinematic tensors. This group of models has been called explicit algebraic stress models (EASM), Gatski and Speziale (1993), Wallin and Johanson (2000), Wallin and Johanson (2002). These models are constructed by representation theorems from the differential equation, using an equilibrium assumption for the advection of the anisotropic Reynolds stress tensor. At what extent does this assumption reflect conditions of real flow and how well these basis tensors physically represent the anisotropic Reynolds stress for complex flows is still being investigated.

With the help of direct numerical simulation (DNS) these group of models can be tested. DNS requires a hardware capacity and memory in order to have a mesh refined enough to capture the small scales, scales of Komolgorov, and give accurate predictions. For this reason, with the hardware capacity of nowadays it is prohibitive the use of DNS in complex flows. However, the data base of simple flows using DNS is important to understand the physics of turbulence and can be used to verify the behavior of the proposed constitutive equations. Some of these non linear models have been already tested for complex flow, for example the flow through a square duct (Mompean et al., 1996), (Mompean, 1998), (Naji et al., 2004) and for the plane channel flow (Schmitt, 2007).

The objective of the present work is to apply tensor decomposition methods onto DNS data in order to have guidelines to construct NLEVM and AESM models. Generally speaking the theorems decompose a tensor \mathcal{V} with respect to another one, \mathcal{U} , in a part which is coaxial and another orthogonal with respect to this second tensor.

2. THEORETICAL ANALYSIS

2.1 Decomposition of a tensor with respect to another

2.1.1 General

Let us consider two second order tensors \mathcal{U} and \mathcal{V} . There is a family of decompositions of tensor \mathcal{V} with respect to \mathcal{U} that is relevant to the present analysis. This family decomposes \mathcal{V} into two additive parts as

$$\mathcal{V} = P_{\mathcal{V}}^{\mathcal{U}} + \tilde{P}_{\mathcal{V}}^{\mathcal{U}} \quad (2)$$

that enjoy the following properties

- i) $P_{\mathcal{V}}^{\mathcal{U}}$ and $\tilde{P}_{\mathcal{V}}^{\mathcal{U}}$ are orthogonal¹.
- ii) \mathcal{U} and $P_{\mathcal{V}}^{\mathcal{U}}$ are coaxial²
- iii) \mathcal{U} and $\tilde{P}_{\mathcal{V}}^{\mathcal{U}}$ are orthogonal.

If \mathcal{U} and \mathcal{V} were first order tensors, there would be an unique pair $\{P_{\mathcal{V}}^{\mathcal{U}}, \tilde{P}_{\mathcal{V}}^{\mathcal{U}}\}$ that could satisfy properties (i)-(iii). Since \mathcal{U} and \mathcal{V} are second order tensors, these properties do not decompose \mathcal{V} in an unique manner. Essentially this happens because it is possible for a second order tensor to commute with and be orthogonal to another one at the same time. A simple example that can illustrate this fact is the pair rate-of-strain tensor, \mathbf{D} , and the identity tensor, $\mathbf{1}$ for the case of an incompressible fluid. The identity tensor commutes with any other tensor and $\text{tr}(\mathbf{D} \cdot \mathbf{1}) = \text{tr}\mathbf{D} = 0$. Therefore, to construct the family of decompositions indicated, we can start from splitting tensor \mathcal{V} into three parts as

$$\mathcal{V} = \varphi_{\mathcal{V}}^{\mathcal{U}+} + \varphi_{\mathcal{V}}^{\mathcal{U}\pm} + \varphi_{\mathcal{V}}^{\mathcal{U}-} \quad (3)$$

where $\varphi_{\mathcal{V}}^{\mathcal{U}+}$ is a part of \mathcal{V} that commutes with, but is not orthogonal to \mathcal{U} , $\varphi_{\mathcal{V}}^{\mathcal{U}\pm}$ commutes with and is orthogonal to \mathcal{U} , and $\varphi_{\mathcal{V}}^{\mathcal{U}-}$ does not commute with but is orthogonal to \mathcal{U} .

Therefore, we can identify, from $\mathcal{V} = \varphi_{\mathcal{V}}^{\mathcal{U}+} + \varphi_{\mathcal{V}}^{\mathcal{U}\pm} + \varphi_{\mathcal{V}}^{\mathcal{U}-}$,

$$\varphi_{\mathcal{V}}^{\mathcal{U}+} \equiv \zeta\mathcal{U}, \quad (4)$$

$$\varphi_{\mathcal{V}}^{\mathcal{U}\pm} \equiv \mathcal{V}_{diag}^{\mathcal{U}} - \zeta\mathcal{U}, \quad (5)$$

$$\varphi_{\mathcal{V}}^{\mathcal{U}-} \equiv \mathcal{V}_{off-diag}^{\mathcal{U}}. \quad (6)$$

Therefore, we come to the conclusion that the pair $\{P_{\mathcal{V}}^{\mathcal{U}}, \tilde{P}_{\mathcal{V}}^{\mathcal{U}}\}$ can assume two forms of decompositions:

$$\{P_{\mathcal{V}}^{\mathcal{U}}, \tilde{P}_{\mathcal{V}}^{\mathcal{U}}\} = \{\varphi_{\mathcal{V}}^{\mathcal{U}+}, \varphi_{\mathcal{V}}^{\mathcal{U}-} + \varphi_{\mathcal{V}}^{\mathcal{U}\pm}\} \quad (7)$$

¹Two tensors \mathbf{A} and \mathbf{B} are orthogonal if (and only if) $\text{tr}(\mathbf{A} \cdot \mathbf{B}^T) = 0$, where tr is the trace operator and the superscript T denotes transposition.

²Two tensors are coaxial if (and only if) they share the same eigenvectors. This condition is satisfied if (and only if) they commute.

or

$$\{\mathbf{P}_v^U, \tilde{\mathbf{P}}_v^U\} = \{\varphi_v^{U+} + \varphi_v^{U\pm}, \varphi_v^{U-}\} \quad (8)$$

Because of the what is stated above these two cases constitute the basis of the present analysis and are explored next.

2.2 The three approaches of the present analysis

2.2.1 Boussinesq hypothesis

The Reynolds stress tensor, \mathbf{R} , is defined through

$$\mathbf{R} = \overline{u'_i u'_j} \mathbf{e}_i \mathbf{e}_j \quad (9)$$

where u'_i are fluctuations of the i -component of the velocity and the over-line, $\overline{(\)}$ indicates the average operation. The Boussinesq hypothesis (Boussinesq, 1877), is based on the assumption that the turbulent shear stress is linearly dependent on the mean velocity gradient. Therefore the structure of the relation between molecular shear stress and kinematics is maintained for the turbulent shear stress, now replacing the rate-of-strain tensor and the molecular viscosity with the mean-rate-of-strain tensor and a "eddy viscosity". Hence, for a 2-D cartesian flow where x is the coordinate along the wall and y is orthogonal to this wall

$$-\overline{u'v'} = \nu_T \frac{\partial U}{\partial y} \quad (10)$$

where ν_T is a "eddy viscosity".

The generalization of this hypothesis was done by Komolgorov (1942). Let us consider tensor \mathbf{b} , the anisotropic Reynolds stress defined as

$$\mathbf{b} = - \left(\mathbf{R} - \frac{1}{3} \text{tr} \mathbf{R} \right) \quad (11)$$

A tensor version of Eq.(10) can be written as

$$\mathbf{b} = 2\nu_T \mathbf{D}, \quad (12)$$

where \mathbf{D} is the symmetric part of the mean velocity gradient. Let us suppose we have obtained the Reynolds stress (and therefore \mathbf{b}) from DNS or experimental data. Let us suppose this same source has provided us with some kinematic information such as the mean velocity profile, and therefore \mathbf{D} .

How can we test if Eq.(12) holds? Or, what is a better approach, how can we quantify how Eq.(12) adheres to the data in a general flow? And how can we obtain ν_T ? The approach used here is to decompose tensor \mathbf{b} into a tensor which is proportional to \mathbf{D} and a tensor \mathbf{D}^\perp which is orthogonal to \mathbf{D} . Hence,

$$\mathbf{b} = \alpha \mathbf{D} + \mathbf{D}^\perp. \quad (13)$$

Taking the inner product of Eq.(13) with respect to \mathbf{D} and imposing that $\text{tr}(\mathbf{D}^\perp \cdot \mathbf{D}) = 0$, we have

$$\alpha = \frac{\text{tr}(\mathbf{b} \cdot \mathbf{D})}{\text{tr}(\mathbf{D} \cdot \mathbf{D})}. \quad (14)$$

Therefore, α is the best scalar that can be related to the turbulent viscosity defined by Eq.(12).

To be consistent with the usual approach in turbulence, the scalar quantity α will be scaled with the turbulent kinetic energy k and dissipation rate ϵ to compose a quantity with the dimension of a viscosity, i.e.

$$\alpha = 2C_\mu \frac{k^2}{\epsilon}, \quad (15)$$

where C_μ is a dimensionless scalar.

An important index of the present analysis is a global measure of how important is the term $\alpha \mathbf{D}$ when compared to \mathbf{b} , in other words, how Komolgorov's Eq.(12) can fit DNS or experimental data.

In the present work, this parameter is given by

$$index_I = 1 - \frac{2}{\pi} \cos^{-1} \left(\sqrt{\frac{\text{tr}(\alpha^2 \mathbf{D}^2)}{\text{tr} \mathbf{b}^2}} \right). \quad (16)$$

2.2.2 How the rate-of-strain tensor can explain the Reynolds stress

A second approach can use the decomposition of the Reynolds stress into a part which is coaxial to \mathbf{D} , Φ_b^D , and another which is orthogonal to \mathbf{D} , $\tilde{\Phi}_b^D$. Mathematically, this is represented by

$$\mathbf{b} = \Phi_b^D + \tilde{\Phi}_b^D. \quad (17)$$

The in-phase part, Φ_b^D , is the part of the Reynolds stress that can be explained by \mathbf{D} . In other words, if the only information we had about kinematics were tensor \mathbf{D} , Φ_b^D is the largest part of the Reynolds stress that could be modelled. Therefore, Φ_b^D captures a larger part of \mathbf{b} than $\alpha\mathbf{D}$ where α is given by Eq.(14). As discussed previously, Φ_b^D can be written as an isotropic function of \mathbf{D} . From the Cayley-Hamilton theorem, it can be shown that Φ_b^D is of the following form

$$\Phi_b^D = \alpha_0 \mathbf{1} + \alpha_1 \mathbf{D} + \alpha_2 \mathbf{D}^2. \quad (18)$$

Using dimensionless quantities for the coefficients, we can write

$$\Phi_b^D = C_I k \mathbf{1} + 2C_D \frac{k^2}{\epsilon} \mathbf{D} + C_{D^2} \frac{k^3}{\epsilon^2} \mathbf{D}^2. \quad (19)$$

Since \mathbf{b} is traceless we have, for an incompressible fluid, that

$$3C_I k + C_{D^2} \frac{k^3}{\epsilon^2} \text{tr} \mathbf{D}^2 = 0. \quad (20)$$

We can also construct a global index to measure the importance of Φ_b^D on \mathbf{b} ,

$$index_{II} = 1 - \frac{2}{\pi} \cos^{-1} \left(\sqrt{\frac{\text{tr} \left[\left(\Phi_b^D \right)^2 \right]}{\text{tr} \mathbf{b}^2}} \right), \quad (21)$$

and this index is also a normalized parameter not less than $index_I$ ($0 \leq index_I \leq index_{II} \leq 1$) since it captures the total influence of \mathbf{D} on the Reynolds stress and not only its linear influence.

2.2.3 The orthogonal part of the rate-of-strain tensor

This step consists on identifying the part of the Reynolds stress that can be explained by the orthogonal to \mathbf{D} tensor

$$\bar{\mathbf{P}} = \mathbf{D} \cdot \bar{\mathbf{W}} - \bar{\mathbf{W}} \cdot \mathbf{D}. \quad (22)$$

In the above equation,

$$\bar{\mathbf{W}} = \mathbf{W} - \Omega^D, \quad (23)$$

where \mathbf{W} is the skew-symmetric part of the mean velocity gradient (the mean vorticity tensor). The overlined \mathbf{W} indicates that this tensor is computed relative to Ω^D , the rate of rotation of the eigenvectors of \mathbf{D} , defined through

$$\Omega^D \equiv \dot{e}_k^D e_k^D, \quad (24)$$

where e_k^D are the normalized eigenvectors of \mathbf{D} , and \dot{e}_k^D are its time derivatives. This symmetric traceless tensor was called by Thompson and Souza Mendes (2005) the persistence-of-straining tensor and appears on representation tensor theorems that represent a general isotropic symmetric tensor as a function of \mathbf{D} and $\bar{\mathbf{W}}$ (Thompson et al., 1999). As shown by Thompson (2008) this tensor captures the first (infinitesimal linear) tendency of a generic flow to depart from a general extensional flow, an extensional motion which is not necessarily a motion with constant stretch history.

In order to develop a frame-invariant algebraic turbulent model Rumsey et al. (2000) have considered the three term basis representation (\mathbf{D} , \mathbf{D}^2 and \mathbf{W}), and replace the rotation rate tensor \mathbf{W} with $\bar{\mathbf{W}}$. Then, they identify the quantity Ω^D measuring the (local) relative angular velocity between the strain rate principal axes and the Cartesian frame base. In the field of viscoelastic flows, Mompean et al. (2003) have also used $\bar{\mathbf{P}}$ as a basis for an algebraic extra-stress constitutive equation.

Obtaining tensor $\bar{\mathbf{P}}$ can be a difficult task since, from Eq.(24), the rate of change of the eigenvectors of \mathbf{D} have to be calculated. This difficulty has sometime made some researchers to use tensor $\mathbf{D} \cdot \mathbf{W} - \mathbf{W} \cdot \mathbf{D}$ instead, although this tensor is non-objective, i.e. depend on the chosen frame of reference.

Here we have used a simpler approach, based on the decomposition of the time derivative of \mathbf{D} into the in-phase and out-of-phase parts, with respect to \mathbf{D} (see Eq.17). Hence,

$$\dot{\mathbf{D}} = \Phi_{\mathbf{D}}^{\mathbf{D}} + \tilde{\Phi}_{\mathbf{D}}^{\mathbf{D}}. \quad (25)$$

The in-phase part can be written as,

$$\Phi_{\mathbf{D}}^{\mathbf{D}} = \mathbf{D}', \quad (26)$$

where \mathbf{D}' is the natural convected time derivative (Thompson, 2008) of \mathbf{D} and the out-of-phase part is given by

$$\tilde{\Phi}_{\mathbf{D}}^{\mathbf{D}} = -(\mathbf{D} \cdot \boldsymbol{\Omega}^{\mathbf{D}} - \boldsymbol{\Omega}^{\mathbf{D}} \cdot \mathbf{D}). \quad (27)$$

Therefore, if we apply the decomposition defined by Eq.(17) and find $\tilde{\Phi}_{\mathbf{D}}^{\mathbf{D}}$, we can find the persistence-of-straining tensor through

$$\bar{\mathbf{P}} = \mathbf{D} \cdot \bar{\mathbf{W}} - \bar{\mathbf{W}} \cdot \mathbf{D} = \mathbf{D} \cdot \mathbf{W} - \mathbf{W} \cdot \mathbf{D} + \tilde{\Phi}_{\mathbf{D}}^{\mathbf{D}}. \quad (28)$$

This approach is more interesting, not only because it comes from a calculation of $\dot{\mathbf{D}}$ but also, because $\boldsymbol{\Omega}^{\mathbf{D}}$ is not always uniquely determined although $\mathbf{D} \cdot \boldsymbol{\Omega}^{\mathbf{D}} - \boldsymbol{\Omega}^{\mathbf{D}} \cdot \mathbf{D}$ is, as discussed by Huilgol (1979).

Since $\bar{\mathbf{P}}$ is orthogonal to \mathbf{D} , we can search for the part of $\tilde{\Phi}_{\mathbf{D}}^{\mathbf{D}}$ that is proportional to $\bar{\mathbf{P}}$. In other words, the decomposition stated by Eq.(17) can be written in another form as

$$\mathbf{b} = \Phi_b^{\mathbf{D}} + \beta \bar{\mathbf{P}} + \tilde{\Phi}_b^{\mathbf{D}} \Big]_c, \quad (29)$$

where $\tilde{\Phi}_b^{\mathbf{D}} \Big]_c = \tilde{\Phi}_{\mathbf{D}}^{\mathbf{D}} - \beta \bar{\mathbf{P}}$ is mutually orthogonal to \mathbf{D} and $\bar{\mathbf{P}}$. The determination of β follows the same lines as Eq.(14), i. e.

$$\beta = \frac{\text{tr} \left[\tilde{\Phi}_b^{\mathbf{D}} \cdot \bar{\mathbf{P}} \right]}{\text{tr} \left[\bar{\mathbf{P}}^2 \right]}. \quad (30)$$

Having found β we are able to define a third index,

$$index_{III} = 1 - \frac{2}{\pi} \cos^{-1} \left(\sqrt{\frac{\text{tr} \left[\left(\Phi_b^{\mathbf{D}} + \beta \bar{\mathbf{P}} \right)^2 \right]}{\text{tr} \mathbf{b}^2}} \right), \quad (31)$$

enjoying the property $0 \leq index_I \leq index_{II} \leq index_{III} \leq 1$.

Similarly to what was done in the previous section, we can construct a dimensionless coefficient, C_β , based on the parameter β . Since tensor $\bar{\mathbf{P}}$ has the same dimension as \mathbf{D}^2 ,

$$\beta = C_\beta \frac{k^3}{\epsilon^2}. \quad (32)$$

3. DNS data for the square duct

The basic flow statistics of the turbulent flow through a straight duct of square cross section at low Reynolds number are available through a number of independent direct simulations of this bounded flow, see e.g. Huser and Biringen (1993), Gavrilakis (1992), Gavrilakis (1993). There is good qualitative agreement in the statistics extracted from these simulations, thus enabling the study of the duct flow with some confidence. The simulation database that will be used in this paper is that obtained by Gavrilakis (1993).

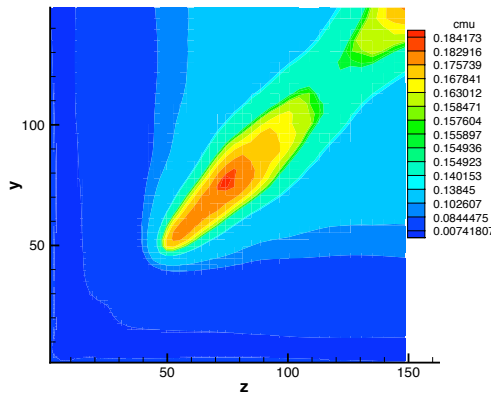


Figure 1. Dimensionless viscosity coefficient on the square duct.

4. RESULTS

4.1 Analysis of the Boussinesq hypothesis

The field of the dimensionless viscosity coefficient,

$$C_\mu = \frac{\alpha}{2} \frac{\epsilon}{k^2}, \quad (33)$$

defined by Eqs.(14) and (15), in the square duct domain is depicted in Fig.1.

The portion of the domain where $C_\mu \approx 0.09$ is coincident to the equilibrium value between production and dissipation. It is known that for wall boundary layers flows, $C_\mu \approx 0.09$ is valid for the region near the wall where production and dissipation are in equilibrium. Some remarks about the equilibrium production and dissipation can be done at this point for the square duct flow. The field of production over dissipation is shown in Fig.(2).

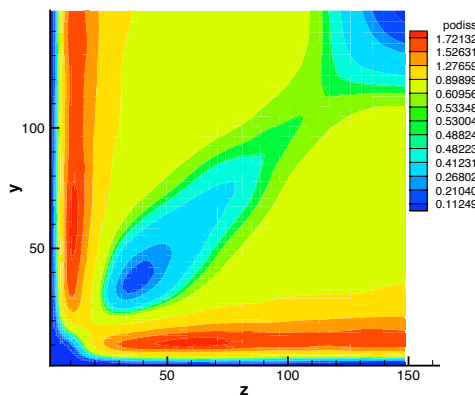


Figure 2. Production over dissipation

We can see that greater values of this quantity are located near the wall, where turbulent dissipation is minimum and the lower values are concentrated near the diagonal line that communicates the corner to the center of duct. We can see that there is a large portion of the domain, labelled in green, where the value of production over dissipation is around unity.

Figure 3 shows the field of $index_I$, a quantification of the part of the anisotropic Reynolds stress tensor that is linear with the rate-of-strain tensor \mathbf{D} .

We can see that there is no part of the domain where this quantity is above 0.5. This result is an indication of the poor predictability of the Boussinesq hypothesis.

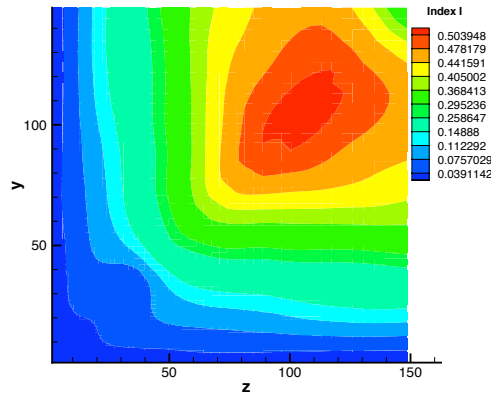


Figure 3. $Index_I$, a measure of how consistent is the hypothesis that the anisotropic Reynolds stress is a linear function of the rate-of-strain tensor on the domain of a square duct.

4.2 Analysis of how in-phase the Reynolds stress is with the deformation rate

In this section, we analyze how the hypothesis that the Reynolds stress is an isotropic function of \mathbf{D} adheres to the DNS data.

Figures 4, 5, and 6 show how \mathbf{b} distributes along $\mathbf{1}$, \mathbf{D} , and \mathbf{D}^2 , respectively, considering its dimensionless coefficients (C_I , C_D and C_{D^2}) as represented by Eq.(19).

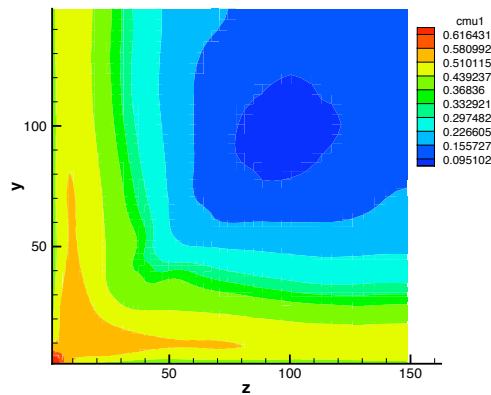


Figure 4. Dimensionless coefficient, C_I , from the in-phase part of the Reynolds stress tensor that multiplies the identity tensor.

Equation (20) was strictly respected, showing that the results obtained by the DNS calculation were solenoidal for the velocity. The differences between C_μ , depicted in Fig.1 and C_D , in Fig.5 are related to the importance of the non-linearity between \mathbf{b} and \mathbf{D} . It can be noticed that the region where its value is around 0.09, characterized by the intersection zone between $z^+ > 120$ and $50 < y^+ < 100$, is almost the same, showing that when production and dissipation equilibrate, the dependence of the Reynolds stress on the rate-of-strain is linear. Figure 7 shows a field of $index_{II}$, a measure of this adherence.

As expected, $index_{II} \geq index_I$ in the whole domain.

4.3 Analysis of the importance of the persistence-of-straining tensor

When the persistence-of-straining tensor $\bar{\mathbf{P}}$ is added to the basis formed by $\mathbf{1}$, \mathbf{D} , and \mathbf{D}^2 , there is a huge portion of \mathbf{b} which becomes explained. This assertion is based on Fig.8, which shows a field of $index_{III}$, that measures the ability of such a basis to capture the Reynolds stress tensor.

This result shows that in almost the entire domain, more than 95% of \mathbf{b} is explained when this basis is added. Also, the lowest value of $index_{III}$ over the square duct domain is 90%.

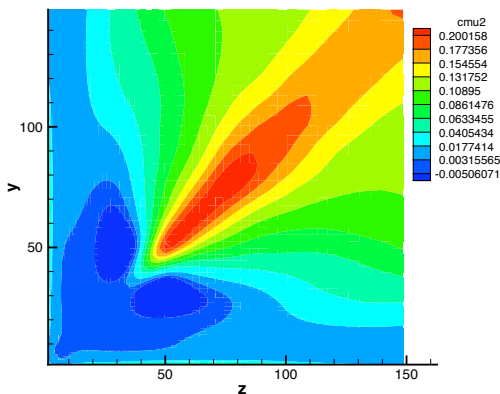


Figure 5. Dimensionless coefficient, C_D , from the in-phase part of the Reynolds stress tensor that multiplies the rate-of-strain tensor.

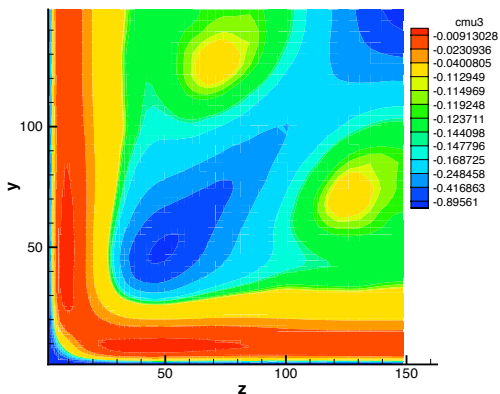


Figure 6. Dimensionless coefficient, C_{D^2} , from the in-phase part of the Reynolds stress tensor that multiplies the square of \mathbf{D} tensor.

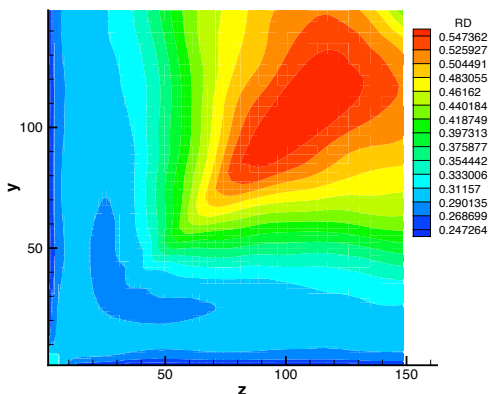


Figure 7. $Index_{II}$, a measure of how consistent is the hypothesis that the anisotropic Reynolds stress is an isotropic function of the rate-of-strain tensor on the domain of a square duct.

5. FINAL REMARKS

We have performed some tensorial filtering on DNS data for the turbulent flow in a square duct. The idea was to gradually progress from a Boussinesq hypothesis where the anisotropic Reynolds stress tensor, \mathbf{b} , is modelled as

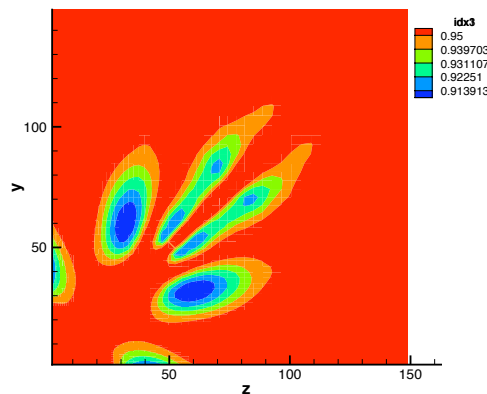


Figure 8. $Index_{III}$, a measure of how consistent is the hypothesis that the anisotropic Reynolds stress is a function of the form $\mathbf{b} = \Phi_b^D + \beta (\mathbf{D} \cdot \overline{\mathbf{W}} - \overline{\mathbf{W}} \cdot \mathbf{D})$ on the domain of a square duct.

a linear function of the rate-of-strain tensor, \mathbf{D} , till a more complete form where the persistence-of-straining tensor $\overline{\mathbf{P}} = \mathbf{D} \cdot \overline{\mathbf{W}} - \overline{\mathbf{W}} \cdot \mathbf{D}$ is used. We have shown that the tensorial basis composed by \mathbf{D} , \mathbf{D}^2 and $\overline{\mathbf{P}}$ is able to almost fully describe the anisotropic Reynolds stress tensor, \mathbf{b} . In the worst region this basis was able to capture 90% of \mathbf{b} as measured by a ratio of its second invariants. On the other hand, the best results for the Boussinesq hypothesis lead to a prediction of only half of the total Reynolds stress, which turns out to be a poor hypothesis in this case. However, when anisotropy is introduced and the Reynolds stress is written as an isotropic function of \mathbf{D} then the ability of prediction increases significantly.

The methodology presented here is simple to be applied to any flow and geometry. Not only DNS, but experimental data can be used as a source for the given analysis. The indexes proposed are able to quantify how linear and non-linear algebraic models for the turbulent stress are in agreement with the data. It is also worth mentioning that this approach is able to determine the best coefficients associated to the respective tensorial basis as a function of the position inside the domain. This important information can be used to construct algebraic models for the closure problem in turbulence.

6. ACKNOWLEDGEMENTS

We would like to acknowledge CNRS, CNPq and FAPERJ for financial support.

7. REFERENCES

- Boussinesq, M., 1877. Essai sur la the'orie des eaux courantes. Mem. pres. Acad. Sci., 3rd edn, Imprimerie Nationale, Paris XXIII, 46.
- Gatski, T. B., Jongen, T., 2000. Nonlinear eddy viscosity and algebraic stress models for solving complex turbulent flows. Progress in Aerospace Sciences 36, 655–682.
- Gatski, T. B., Speziale, C. G., 1993. On explicit algebraic stress models for complex turbulent flows. J. Fluid Mech. 254, 59–78.
- Gavrilakis, S., 1992. Numerical simulation of low-reynolds-number turbulent flow through a straight square duct. J. Fluid Mech. 244, 101–116.
- Gavrilakis, S., 1993. Turbulent velocity structures derived from pod analyses. Institut de Machines Hydrauliques et de Mécanique des Fluides, École Polytechnique Fédérale de Lausanne. Report T-93-30, C134–C156.
- Huilgol, R. R., 1979. Viscoelastic fluid theories based on the left cauchy-green tensor history. Rheol. Acta 18, 451–455.
- Huser, A., Biringen, S., 1993. Direct numerical simulation of turbulent flow in a square duct. J. Fluid Mech. 257, 65–77.
- Lumley, J. L., 1970. Toward a turbulent constitutive relation. J. Fluid Mech. 41, 413–434.

- Mompean, G., 1998. Numerical simulation of a turbulent flow near a righ-angled corner using the Speziale nonlinear model with RNG $k - \epsilon$ equations. *Computers and Fluids* 27, 847–859.
- Mompean, G., Gavrilakis, S., Machiels, L., Deville, M., 1996. On predicting the turbulence-induced secondary flows using non-linear $k - \epsilon$ models. *Phys. Fluids* 8, 1856–1868.
- Mompean, G., Thompson, R. L., Souza Mendes, P. R., 2003. A general transformation procedure for differential viscoelastic models. *J. Non-Newtonian Fluid Mech.* 111, 151–174.
- Naji, H., Mompean, G., El Yahyaoui, O., 2004. Evaluation of explicit algebraic stress models using direct numerical simulations. *Journal of Turbulence* 5, 038, 1–25.
- Pope, S., 1975. A more general effective-viscosity hypothesis. *J. Fluid Mech.* 72, 331–340.
- Rumsey, C. L., Gatski, T. B., Morrison, J. H., 2000. Turbulence model predictions of strongly curved flow in a U-duct. *AIAA Journal* 38 (8), 1394–1402.
- Schmitt, F. G., 2007. Direct test of nonlinear constitutive equation for simple turbulent shear flows using dns data. *Communications in Nonlinear Science and Numerical Simulation* 12, 1251–1264.
- Speziale, C. G., 1987. On non-linear $k-l$ and $k-\epsilon$ models of turbulence. *J. Fluid Mech.* 178, 459–475.
- Thompson, R. L., 2008. Some perspectives on the dynamic history of a material element. *Int. J. Engng. Sci* 46, 524–549.
- Thompson, R. L., Souza Mendes, P. R., 2005. Persistence of straining and flow classification. *Int. J. Engng. Sci* 43 (1-2), 79–105.
- Thompson, R. L., Souza Mendes, P. R., Naccache, M. F., 1999. A new constitutive equation and its performance in contraction flows. *J. Non-Newt. Fluid Mech.* 86, 375–388.
- Wallin, S., Johanson, A. V., 2000. An explicit algebraic reynolds stress model for incompressible and compressible turbulent flows. *J. Fluid Mech* 403, 89–132.
- Wallin, S., Johanson, A. V., 2002. Modelling streamlines curvature effects in explicit algebraic reynolds stress turbulence model. *International Journal of Heat and Fluid Flow* 23, 721–730.

8. Responsibility notice

The author(s) is (are) the only responsible for the printed material included in this paper